Constraints on a massive Dirac neutrino model

Thomas Wynter* and Lisa Randall
Massachusetts Institute of Technology, Cambridge, Massachusetts 02139
(Received 1 June 1993; revised manuscript received 27 January 1994)

We examine constraints on a simple neutrino model in which there are three massless and three massive Dirac neutrinos and in which the left-handed neutrinos are linear combinations of doublet and singlet neutrinos. We examine constraints from direct decays into heavy neutrinos, indirect effects on electroweak parameters, and flavor-changing processes. We combine these constraints to examine the allowed mass range for the heavy neutrinos of each of the three generations.

PACS number(s): 14.60.Pq, 13.20.−v, 13.35.−r

I. INTRODUCTION

Many models of neutrinos have been proposed to accommodate light or massless neutrinos. In a model with no right-handed neutrinos, it is clear that neutrinos are massless. However, if there exist additional states which can play the role of Dirac partners to the left-handed states, it is perplexing why neutrinos should be massless, or at least much lighter than their charged counterparts. Of course, neutrinos can be given small masses by coupling them to the standard Higgs doublet with an extremely small Yukawa coupling, but it is more compelling to have an explanation for their small mass. A common explanation is the so-called "seesaw" mechanism, in which the neutrinos remain light because the additional right-handed states have a large Majorana mass. In such a model, neutrino masses are naturally small, since they are suppressed by the ratio of Dirac to Majorana masses, which is generally taken to be small.

In this paper, we consider another viable alternative (see, for example, [1–3]). In addition to the three "right-handed" neutrinos, there are three additional singlet particles. A lepton symmetry is imposed so that the only allowed mass terms are Dirac masses coupling the right-handed neutrino to the standard left-handed neutrino and to the additional singlet states. The consequence is that there are three heavy Dirac neutrinos, with mass determined primarily by the large mass term connecting the singlet and right-handed neutrinos and three exactly massless neutrinos, the states orthogonal to the massive ones. Such a model has been considered before in several contexts; most recently it has been considered in the context of an extended technicolor model with a Glashow-Iliopoulos-Maiani (GIM) mechanism [3]. In this type of model, the additional neutrino states could be quite light, on the order of 1 GeV.

However, there are many constraints on such neutrinos. They are constrained from direct searches for particles which have them in their final state, by universality constraints, and by flavor-changing constraints. Cosmological arguments are often used to constrain neutrino masses, but the neutrinos of this model are unstable, and so they are not relevant. In this paper, we put the relevant constraints together, making reasonable assumptions on the form of the mass matrix and mixing angles, to determine the allowed parameter regime. Many of these constraints apply quite generally to any model in which the left-handed neutrinos mix with singlet states. Similar bounds were considered in Ref. [4]. This paper updates the bounds, integrates them with those from the CERN e^+e^- collider LEP, and incorporates flavor-changing bounds. We find that, with reasonable assumptions described below, the lightest neutrino can be as light as 2 GeV, although the third-generation neutrino should be much heavier, greater than 80 GeV.

The organization is as follows. We first present the model and describe the approximations which we use to reduce the parameter space. We then consider constraints from meson and Z decays. Following this, we discuss the constraints from the fact that G_F will not have the same relation to standard model parameters when the muon cannot decay to the heavy neutrino state. We then look at flavor-changing processes, which are in general permitted when no flavor symmetries are assumed. However, we assume mixing angles similar to those of the standard Kobayashi-Maskawa (KM) matrix, and so there are approximate U(1) symmetries present. We then put together the constraints and consider three models which describe the ratio of masses of the heavy neutrinos to determine the allowed parameter regime. Finally, we conclude.

II. MODEL AND SIMPLIFYING ASSUMPTIONS

Many models have incorporated the neutrino scenario we discuss here. For example, it has been incorporated into grand unified theory (GUT) models [1,2]. More recently, it has been shown how to incorporate such a model in an extended technicolor scenario [3]. We only consider the phenomenology of the lepton sector here, and so we neglect the origin of the model and focus on the neutrinos.

The standard model is extended by introducing three new left-handed neutrinos S_L and three right-handed neutrinos ν_R. Both left-handed neutrinos are coupled to the right-handed neutrinos through Dirac matrices. All

*Current address: Ecole Normale Supérieure, 24 Rue Lhomond, 75231 Paris Cedex 05, France.

other possible mass entries are forbidden by a lepton number symmetry. Thus

$$-\mathcal{L}_{\text{mass}}=(\nu_R 0)\begin{pmatrix} D & S \\ 0 & 0 \end{pmatrix}\begin{pmatrix} \nu_L \\ S_L \end{pmatrix}+\text{H.c.} \tag{1}$$

This coupling results in three massive Dirac neutrinos and three massless eigenstates. The mass matrices D and S have different mass scales. The scale for D is constrained by SU(2) symmetry breaking whereas the scale for S is not, and so it is reasonable to expect the masses in S to be larger.

The mass of the heavy neutrinos is essentially determined by S. The electron, μ and τ neutrinos are a superposition of massless and massive eigenstates. The mixing to the massive neutrinos will, however, be small; it will be of the order of M_D/M_S, where M_D and M_S are typical masses in D and S, respectively. To see more precisely how this mixing occurs, we need to find the three massless eigenstates ν^0 as well as the three with mass ν^H. The mass matrix can be diagonalized by multiplying on the left and the right by unitary matrices:

$$\begin{pmatrix} V & 0 \\ 0 & 0 \end{pmatrix}\begin{pmatrix} D & S \\ 0 & 0 \end{pmatrix}U=\begin{pmatrix} 0 & 0 \\ 0 & M \end{pmatrix}\text{ with }\begin{pmatrix} \nu_L \\ S_L \end{pmatrix}=U\begin{pmatrix} \nu^0 \\ \nu^H \end{pmatrix}. \tag{2}$$

The unitary matrix V diagonalizes $DD^\dagger+SS^\dagger$ to give M^2. The unitary matrix U is given by

$$U=\begin{pmatrix} U_D^\dagger\Lambda_S V'^\dagger & U_D^\dagger\Lambda_D V'^\dagger \\ U_S^\dagger\Lambda_D V'^\dagger & -U_S^\dagger\Lambda_S V'^\dagger \end{pmatrix}, \tag{3}$$

where the matrices, V', U_D, and U_S are unitary matrices. They diagonalize $M^{-1}VD$ and $M^{-1}VS$ (where M^{-1} is the inverse of the diagonal mass matrix M) to give the diagonal matrices Λ_D and Λ_S:

$$V'^\dagger(M^{-1}VD)U_D^\dagger=\Lambda_D \tag{4}$$

$$V'^\dagger(M^{-1}VS)U_S^\dagger=\Lambda_S\ . \tag{5}$$

The fact that the same V' appears on the left for both these diagonalizations is a consequence of the fact that the two matrix products $M^{-1}VDD^\dagger V^\dagger M^{-1}$ and $M^{-1}VSS^\dagger V^\dagger M^{-1}$ commute with each other, which follows in turn from the fact that their sum is the unit matrix. The most important part of U is the top right 3×3 block $U_D^\dagger\Lambda_S V'^\dagger$ which links the electron, μ, and τ neutrinos to the massive neutrinos ν^H.

To extract bounds on the mass scales of S and D we need to make some simplifications to reduce the number of parameters. We will make the simplification that the matrices D and S are diagonalized by the same unitary matrices. In this case $V'=I_{3\times3}$. If we then redefine the fields S_L by a unitary transformation, absorbing the unitary matrix U_S, we can rewrite the matrix U as

$$U=\begin{pmatrix} U_D^\dagger\Lambda_S & U_D^\dagger\Lambda_D \\ \Lambda_D & \Lambda_S \end{pmatrix}, \tag{6}$$

with $\Lambda_D^2+\Lambda_S^2=I_{3\times3}$.

In this model the mass scale of the Dirac mass S is assumed to be much higher than the scale of the Dirac mass D. If this difference is sufficiently large, we can make the further simplification that $\Lambda_S=I_{3\times3}$. From here on the subscript D on Λ_D will be dropped.

At this point, we will have a large number of parameters. We simplify by assuming that the matrix U_D is similar in structure to the KM matrix for quarks. We note that if there were no singlet left-handed neutrinos S_L the matrix U_D would be the lepton equivalent of the KM matrix in the quark sector. We take the individual elements to be of the same magnitude as those of the KM matrix for quarks. With no further input, this is probably the least arbitrary assumption to make.

We will use these approximations from now on. They leave six free parameters: M_i, the masses of the heavy neutrinos, and M_{D_i}, the masses induced by the mass matrix D which are defined as $M_{D_i}=\Lambda_i\times M_i$. In the following sections we will use experimental results to put limits on these masses.

III. DIRECT SEARCHES FOR HEAVY NEUTRINOS

Many searches for massive neutrinos have already been conducted. Massive neutrinos have been sought in the decays of π^+ [5–10], K^+ [6,7,11], and charmed mesons [12–15], as well as in the neutral current production of neutrino-antineutrino pairs from e^+e^- [16–18] collisions and, more recently the decay of the Z [19,20].

A. Meson decays

If it is kinematically allowed, any process involving the production of doublet neutrinos will be a source of heavy neutrinos. The creation process, however, will be suppressed since the weak eigenstate neutrinos contain only a small mixing of the heavy neutrinos. Leptonic decays of mesons are thus one place to look for heavy neutrinos.

At the lower end of the mass scale heavy neutrino creation in the decay of π^+ mesons has been investigated in Refs. [5–10], and those of K^+ mesons in Refs. [6,7,11]. These experiments attempted to measure the mass of any heavy neutrino as it was created. This was achieved by stopping the π^+ and K^+ mesons and observing the energy of positrons emitted in their decay. The method did not rely on any assumptions about how the heavy neutrinos decayed. For massive neutrinos with masses less than 300 MeV these experiments placed strict limits on the mixings $|U_{ei}|^2$ and $|U_{\mu i}|^2$ of a heavy neutrino ν_i^H into the electron and μ neutrinos. For a range of masses the matrix elements $|U_{ei}|^2$ and $|U_{\mu i}|^2$ were constrained to be less than 10^{-6}. Since we assume the matrix U_D is almost diagonal, we can get direct bounds on Λ_1 and Λ_2 of $\Lambda_1<10^{-3}$ for the mass range 35–400 MeV and $\Lambda_2<10^{-3}$ for the mass range 180–360 MeV (see Figs. 1 and 2).

Further limits on $|U_{ei}|^2$ and $|U_{\mu i}|^2$ come from the decays of charmed D mesons [13–15] [see Figs. 1 curve (e) and 2 curve (d)]. Although similar searches can in principle be performed with decays of the B, they have not yet been done. In total the limits from meson decays, with a few gaps, restrict $\Lambda_1<10^{-3}$ for the mass range 35

MeV–2 GeV and $\Lambda_2 < 10^{-3}$ for the mass range 180 MeV–2 GeV. For much of these ranges the bounds are much stricter than this.

B. e^+e^- Collisions at low c.m. energy

Heavy neutrino-antineutrino pairs would be created by weak interaction currents in e^+e^- annihilations, but since the center-of-mass energy of these collisions is less than the W and Z mass the cross section for the creation of these neutrinos is extremely small. Experiments [16–18] were aimed at detecting the decay of a heavy fourth-generation neutrino and they thus made the assumption that the heavy neutrino had the same coupling to the Z and W as the other neutrinos. This is not the case for the model studied in this paper where each heavy neutrino introduces a mixing angle factor of $|U_{li}|^2$ into the weak interaction couplings. Reinterpreting the data of these experiments including the extra mixing angles results in constraints that are negligible in comparison to the other bounds studied in this paper.

C. Z decays

Massive neutrinos, lighter than M_Z, would also be created in Z decays, and experiments [19,20] have already conducted searches for heavy isosinglet neutrinos, the type discussed in this paper. The most abundant supply of heavy neutrinos would come from the decay of a Z into one heavy neutrino and one massless neutrino. For a Z decaying into a heavy neutrino ν_i^H (lighter than the Z) and any of the three massless antineutrinos ν_j^0 the creation is suppressed by

$$R_i = \sum_{j=1}^{3} \left| \sum_{l=e,\mu,\tau} U_{jl}^{\dagger} U_{l(i+3)} \right|^2 = \Lambda_i^2 , \tag{7}$$

where R_i has the following meaning: If N is the number of neutrinos (from one family of the standard model) created in the experiment, then the number of heavy neutrinos ν_i^H created is $R_i N$.

Experiments aim to detect the neutrino by its decay. The decay of the neutrino would be quite distinctive. In general, it will decay to a high energy lepton and a virtual W or Z, which would then decay into leptons, or hadrons if the neutrino is massive enough. The total decay rate can be written in terms of the rate for muon decay as [4]

$$\Gamma(\nu_i^H \to \text{leptons/hadrons}) = \sum_l |U_{l(i+3)}|^2 \left[\frac{M_i}{M_\mu} \right]^5 \Phi_l(M_i) \times \Gamma(\mu \to e\nu\bar{\nu}) , \tag{8}$$

where $\Phi_l(M_i)$ is a factor that weights the decay rate for a single channel by the effective number of channels into which there is sufficient energy to decay and takes into account the different Feynman diagrams.

There are two reasons why decays like this might not have been seen in experiments.

Very few heavy neutrinos are produced. If we assume that nearly all the neutrinos decay inside the detector, then the fraction R_d that decay inside the detector is given by

$$R_d = R_i = \Lambda_i^2 .$$

If R_i is sufficiently small, no neutrinos would be detected.

The neutrinos have a long lifetime. If the neutrinos are light, they could have a very long lifetime and thus decay

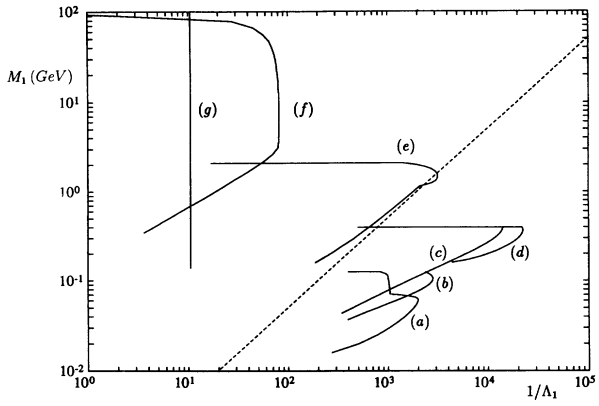

FIG. 1. Bounds placed on the heavy neutrino masses by considering all the constraints in Secs. III and IV. The plot is of the neutrino mass M_1 against the ratio $1/\Lambda_1 = M_1/M_{D_1}$. Any region to the left of a solid line is forbidden by experiment. The dashed line is the line along which the mass M_{D_1} is equal to the electron mass. Regions excluded come from (a) Ref. [8], massive neutrinos in pion decays; (b), (c), (d) Ref. [6], massive neutrinos in pion and kaon decays; (e) Ref. [13], massive neutrinos in D meson decays; (f) Ref. [19], Secs. III C, Z decays; (g) Sec. IV D, branching ratio $\Gamma(\pi \to e\nu)/\Gamma(\pi \to \mu\nu)$.

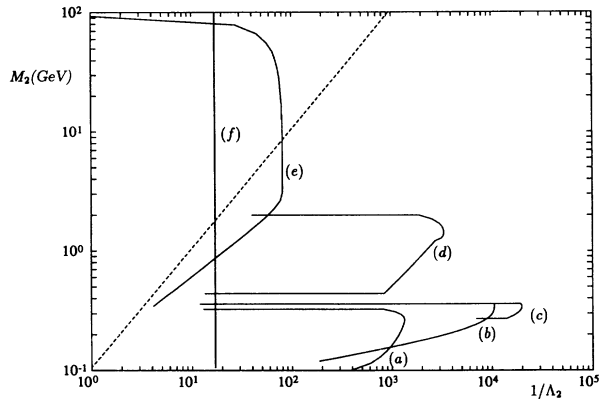

FIG. 2. Bounds placed on the heavy neutrino masses by considering all the constraints in Secs. III and IV. The plot is of the neutrino mass M_2 against the ratio $1/\Lambda_2 = M_2/M_{D_2}$. Any region to the left of a solid line is forbidden by experiment. The dashed line is the line along which the mass M_{D_2} is equal to the μ mass. Regions excluded come from (a) Ref. [11], massive neutrinos in kaon decays; (b), (c) Ref. [6], massive neutrinos in kaon decays; (d) Ref. [13], massive neutrinos in D meson decays; (e) Ref. [19], Sec. III C, Z decays; (f) Sec. IV B, changes in G_F.

almost entirely outside of the detector.

We can then calculate the fraction R_d of Z's that would decay inside the detector:

$$R_d = R_i \left[1 - \exp\left[\frac{S_d}{c} \gamma^{-1} \Gamma(\nu_i^H \rightarrow \text{leptons/hadrons}) \right] \right] , \tag{9}$$

where γ is the time dilation factor due to the relativistic motion of the neutrino, and for $M_Z \gg M_i$ is given by $\gamma = M_Z/2M_i$; S_d is the size of the detector and c is the speed of light.

The experiment of Ref. [19] involved a search through 4×10^5 hadronic Z decays and placed limits of $\Lambda_i < 0.014$ over the range 5–50 GeV. Above 50 GeV the phase space for heavy neutrino production becomes smaller and the limits placed on the Λ_i become less strict. Below 5 GeV the limits are reduced due to the long lifetime of the neutrinos. In Figs. 1, curve (g), 2, curve (e), and 3, curve (b), are marked out the forbidden regions in the M_i, $1/\Lambda_i$ plane for the three heavy neutrinos.

IV. CHANGES IN WEAK INTERACTION DECAYS AND PARAMETERS

Aside from direct searches for the heavy neutrino, the existence of the heavy neutrino will affect precision measurements of various electroweak processes. This can be the case because G_F will no longer have the standard model relation to $\sin\theta_W$, since the μ decay rate will be different if the μ cannot decay into the heavy neutrino. This would change the relation between precisely measured electroweak parameters, for example, the W mass or $\sin^2\theta_W$ as measured in the forward-backward asymmetry. Furthermore, it would lead to an apparently nonunitary KM matrix.

Further constraints come from pion decay branching ratios if the heavy electron or μ neutrinos are heavier than the pion. Similarly universality could be violated and would be seen in τ decay. Finally, the Z width can be affected, both indirectly through a change in the extracted $\sin^2\theta$, and directly if the neutrinos are heavier than the Z.

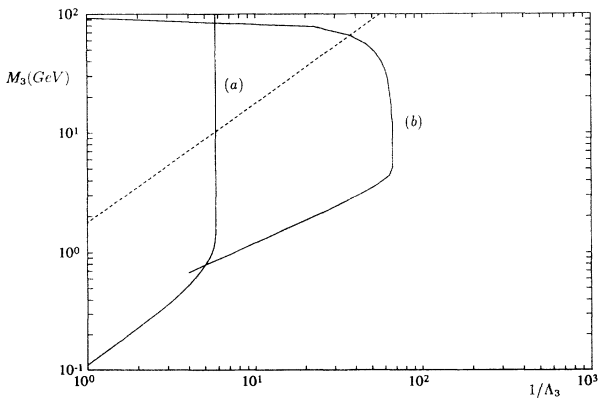

FIG. 3. Bounds placed on the heavy neutrino masses by considering all the constraints in Secs. III and IV. The plot is of the neutrino mass M_3 against the ratio $1/\Lambda_3 = M_3/M_{D_3}$. Any region to the left of a solid line is forbidden by experiment. The dashed line is the line along which the mass M_{D_3} is equal to the τ mass. Regions excluded come from (a) Sec. IV E, τ decays; (b) Ref. [19], Sec. III C, Z decays.

A. μ decays and the Fermi coupling constant G_F

The Fermi coupling constant G_F is the effective coupling constant for four-Fermi interactions and is measured extremely accurately from μ decays. If the mass of the massive neutrinos is greater than that of the μ, the decay width for the μ would be decreased, since it would not be able to decay into the heavy neutrinos; this in turn would lead to a change in the predicted value of G_F.

Specifically,

$$(G_F)^2_{\text{new}} = \sum_{i,j=1}^{3} |U_{ei} U^{\dagger}_{j\mu}|^2 (G_F)^2_{\text{old}} , \tag{10}$$

which leads to

$$\delta(G_F)^2_{\text{muon decays}} \simeq -(\Lambda_1^2 + \Lambda_2^2) , \tag{11}$$

where δ means the fractional change. Of course, G_F is a measured number. What we mean here is the change in the coefficient of the four-Fermi operator which yields μ decay.

B. Semileptonic decays and the KM matrix

The estimates of the semileptonic processes would also be affected but to a lesser extent. The same value of G_F is also used for the effective coupling constant for semileptonic decays, where elements of the KM matrix are determined. One would expect these elements to be part of a unitary matrix.

The important point to consider is that the effective coupling constants for the leptonic and semileptonic four-Fermi interactions would no longer be the same, and if it was assumed that they were, the predicted matrix elements for the KM matrix would no longer be those of a unitary matrix. We can check the unitarity of the KM matrix by looking at the matrix elements $(\text{KM})_{ud}$, $(\text{KM})_{us}$, and $(\text{KM})_{ub}$; the sum of their square magnitudes must add up to 1. The effect of having heavy neutrinos would be to make this sum slightly bigger than 1. The most important shift will come from the change in nuclear β decays used to determine the $(\text{KM})_{ud}$ element. Consequently, what must be compared are the changes in the value of G_F and in the rates for nuclear β decays.

Specifically, as above,

$$(G_F)^2_{\text{new}} = \sum_{i,j=1}^{3} |U_{ei} U^{\dagger}_{j\mu}|^2 (G_F)^2_{\text{old}} , \tag{12}$$

which leads to

$$\delta(G_F)^2 \mu_{\text{decays}} \simeq -(\Lambda_1^2 + \Lambda_2^2) \tag{13}$$

and similarly

$$\delta(\beta \text{ decay}) \simeq -\Lambda_1^2 , \tag{14}$$

where δ means the fractional change. The fractional change in the width of the μ minus the fractional change in nuclear β decays must be less than the experimental uncertainty in the sum of the matrix elements. From Ref. [21],

$$|(\mathrm{KM})_{ud}|^2+|(\mathrm{KM})_{us}|^2+|(\mathrm{KM})_{ub}|^2 = 1(+8.6\times10^{-4},-4.7\times10^{-3}) . \quad (15)$$

This leads to $\Lambda_2<6\times10^{-2}(2\sigma)$ if the neutrinos are heavier than the μ. The resulting bound is plotted in Fig. 2, curve (f).

C. M_W and $\sin\theta_W$

Changes in G_F would also affect the prediction of other weak interaction parameters. The ratio of the mass of the W and Z, for example, depends upon G_F. Specifically (using the notation of Ref. [21]),

$$\frac{M_W^2}{M_Z^2}=\frac{1}{2}\left[1+\left[1-\frac{4\pi\alpha(1+\delta v)}{\sqrt{2}M_Z^2G_F}\right]^{1/2}\right] , \quad (16)$$

where δv is a radiative correction parameter much less than 1. Using the above the change in the predicted value of M_W/M_Z due to the change in G_F is

$$\delta(M_W/M_Z)=0.088\times\delta(G_F) . \quad (17)$$

Current experimental bounds [22] place $\delta(M_W/M_Z)<7.7\times10^{-3}(2\sigma)$ which gives a bound for G_F of

$$\delta(G_F)<8.8\times10^{-2}(2\sigma) . \quad (18)$$

In fact this bound is too strong due to the uncertainty in the top quark mass. However, since it is less strict than the bound coming from the KM matrix, it will not be incorporated.

The Weinberg angle $\sin^2\theta_W$ also depends on G_F [the on-shell definition is $\sin^2\theta_W=(1-M_W^2/M_Z^2)$ and this can be compared with the forward-backward asymmetry of the process $e^+e^-\to f\bar{f}$, which depends on θ_W]. However, this too is weaker than the constraint from the unitarity of the KM matrix.

D. Pion decay branching ratios

The ratio of the two decay channels for a $\pi^\pm$, $\pi\to e\nu_e$ and $\pi\to\mu\nu_\mu$, provides another bound [4]. In this model,

$$\frac{\Gamma(\pi\to e\nu_e)}{\Gamma(\pi\to\mu\nu_\mu)}=1.2345\times10^{-4}\left[1-\sum_{i=4}^{6}(|U_{ei}|^2-|U_{\mu i}|^2)\right] , \quad (19)$$

where the factor 1.2345×10^{-4} is the theoretical value of the ratio in the standard model (Marciano, in [23]; see also [24,25]). The mixing angle factors apply for neutrinos too heavy to be produced. Experimentally the ratio is known to be $(1.2346\pm0.0035\pm0.0036)\times10^{-4}$ [23,26]. Using the fact that U_D is almost diagonal and that $\Lambda_2<6\times10^{-2}$ leads to

$$0.041>(\Lambda_1^2-\Lambda_2^2)\Longrightarrow\Lambda_1<0.095(2\sigma) . \quad (20)$$

The resulting bound is displayed in Fig. 1, curve (f).

E. τ decays

If the neutrinos are all heavier than the τ then the decay width of the τ would also be affected. As for the case of the μ decay it can be shown that the partial width $\Gamma(\tau\to e\nu_\tau\nu_e)$ would be reduced by $\sim(\Lambda_1^2+\Lambda_3^2)$ and the partial width $\Gamma(\tau\to\mu\nu_\tau\nu_\mu)$ would be reduced by $\sim(\Lambda_2^2+\Lambda_3^2)$. Consequently, the partial width for decay into leptons would be reduced by

$$\sim(\tfrac{1}{2}\Lambda_1^2+\tfrac{1}{2}\Lambda_2^2+\Lambda_3^2) . \quad (21)$$

This fractional change minus the fractional change in the width for μ decay must be less than the experimental uncertainty of the partial width for the τ. This gives a further bound on the Λ_i:

$$|\tfrac{1}{2}\Lambda_1^2+\tfrac{1}{2}\Lambda_2^2-\Lambda_3^2|\le0.015(1\sigma) , \quad (22)$$

where the uncertainty in the partial width of the τ is 1.5% [21]. To obtain a bound for Λ_3^2 we use the following formula for calculating the error at the 1σ level of a sum of terms each with their own errors:

$$\Lambda_3^2=[(\tfrac{1}{2}\Lambda_1^2)_{1\sigma}^2+(\tfrac{1}{2}\Lambda_2^2)_{1\sigma}^2+0.015^2]^{1/2} , \quad (23)$$

where, at the 1σ level, we use the bounds from the previous section $\Lambda_1^2<0.0045$ and $\Lambda_2^2<0.0018$. This leads to a bound on Λ_3 at the 2σ level of

$$\Lambda_3<0.17(2\sigma) . \quad (24)$$

The resulting bound is plotted in Fig. 3, curve (a).

F. Width of the Z

For neutrinos heavier than the Z the width will be reduced, since the decay into the heavy neutrinos will no longer be kinematically allowed. Experimentally, the partial width $\Gamma_{\nu\bar{\nu}}$ of the Z is known to an accuracy of 1.8% [27]. In this model,

$$\Gamma_{\nu\bar{\nu}}\propto\frac{1}{3}\sum_i|1-\Lambda_i^2|=1-\frac{1}{3}\sum_i\Lambda_i^2 , \quad (25)$$

where the sum over i is only over neutrinos heavier than the Z. This gives the bound

$$\sum_i\Lambda_i^2<0.108(2\sigma) . \quad (26)$$

There is also an effect if μ decay is changed. However, it is not numerically as important.

In Figs. 1, 2, and 3 are plots of the bounds placed on the Λ_i by all the processes considered in Secs. III and IV.

V. LEPTON FLAVOR-CHANGING PROCESSES

Flavor-changing processes were also examined in this model. These processes are exactly analogous to flavor-changing processes in the quark sector. Three processes with strong experimental bounds were considered: (i) $\mu\to e\gamma$; experimentally: $\Gamma(\mu\to e\gamma)/\Gamma(\mu\to e\nu\bar{\nu})<5\times10^{-11}$ [28], (ii) $\mu\to ee^+e^-$; experimentally: $\Gamma(\mu\to ee^+e^-)/\Gamma(\mu\to e\nu\bar{\nu})<10^{-12}$ [29], and (iii) $\mu\mathrm{Ti}\to e\mathrm{Ti}$; experimentally: $\Gamma(\mu\mathrm{Ti}\to e\mathrm{Ti})/\Gamma(\mu^-\mathrm{Ti}$ capture)

$<5\times10^{-12}$ [30], where the bounds are given at the 90% confidence level. These processes can only occur via loop diagrams involving the exchange of virtual neutrinos. The couplings of the neutrinos to the μ and the electron involve the unitary matrix U; specifically, the neutrino-W-μ vertex includes a mixing angle $U^{\dagger}_{i\mu}$ for coupling to the ith neutrino, and the mixing angle U_{ei} is included with the neutrino-W-electron vertex. The amplitudes are obtained by summing over all intermediate states i. All terms proportional to the sum $\sum_{i=1}^{6} U_{ei}U^{\dagger}_{i\mu}$ are automatically canceled since U is unitary. This is the GIM mechanism. It is an analogue of the strong suppression of neutral current flavor-changing processes in the quark sector. Notice this is independent of the approximations we made. In all cases there is very strong GIM suppression.

For the purpose of calculations, the masses of the electron, μ, and τ and the mass matrix D are generated in the standard way by coupling to the Higgs boson, so that the loops involved charged Higgs bosons. 't Hooft gauge is used throughout, simplifying the form of the propagators and setting the masses of the W and the charged Higgs bosons to be the same. We will now consider, in detail, the three flavor-changing processes.

A. $\mu\rightarrow e\gamma$

This process has been investigated previously; see Refs. [31,32]. Below we will give an outline of the calculation for the general case, where the neutrino masses are not assumed to be less than M_W. To simplify the calculations the electron is taken to be massless. The general form of the amplitude is constrained by gauge invariance; thus, the gauge-invariant form of the amplitude with a massless electron is given by

$$\langle e,\gamma|(S-1)|\mu\rangle = A\bar{u}_e[(1-\gamma_5)ik^{\nu}\epsilon^{\lambda}\sigma_{\lambda\nu}i\partial\!\!\!/]u_{\mu} , \quad (27)$$

where k is the photon four-momentum, ϵ is the polarization of the photon, and A is a constant to be determined. The partial derivative term is included to ensure that, in the hypothetical case where the μ mass goes to zero, only the left-handed component of the μ coupled to the W is involved in the decay. The amplitude can then be rewritten using the Gordon decomposition as

$$\langle e,\gamma|(S-1)|\mu\rangle = Am_{\mu}\bar{u}_e[(1-\gamma_5)(2\epsilon\cdot p - m_{\mu}\epsilon\!\!\!/)\,u_{\mu} , \quad (28)$$

where m_{μ} is the μ mass and p is the four-momentum of the incoming μ. To simplify the calculation, only the terms proportional to $\epsilon\cdot p$ need to be calculated. In principle there are eight possible diagrams contributing (see Fig. 4). Diagrams (5)–(8) contain only the $\epsilon\!\!\!/$ term and thus can be ignored. They will cancel with similar terms coming from the first four diagrams.

In evaluating diagrams (1)–(4) we can define a factor I^i_j for each of the diagrams $i=(1)$–(4), and for each of the massive neutrinos $j=1$–3. I^i_j is the contribution from the massive neutrino ν_j minus the contribution from a massless neutrino. Summing over the three massive neutrinos j the contribution of diagram i to the constant A is

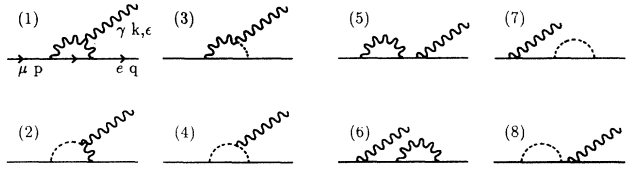

FIG. 4. Feynman diagrams for the flavor changing process $\mu\rightarrow e\gamma$, Sec. V A. The dotted lines correspond to charged Higgs bosons.

$$-iK\sum_{j=1}^{3} U_{D_{ej}}U^{\dagger}_{D_{j\mu}}\Lambda_j^2 I_j^i/(32\pi^2M_W^2) , \quad (29)$$

where $K=-e^3/(2\sin^2\theta_W)$. We can also define the sum

$$I_{\mu e}=\sum_{i=1}^{4}\sum_{j=1}^{3} U_{D_{ej}}U^{\dagger}_{D_{j\mu}}\Lambda_j^2 I_j^i , \quad (30)$$

so that the total contribution to the constant A from all the diagrams is

$$-iKI_{\mu e}/(32\pi^2M_W^2) . \quad (31)$$

Performing the calculations gives the following results for the I^i_j:

$$I_j^1=-[a_j(a_j^2-3a_j+\tfrac{31}{12})-\tfrac{7}{12}+a_j^3(a_j-\tfrac{3}{2})\delta_j^2\ln\delta_j] , \quad (32)$$

$$I_j^2=-[\tfrac{1}{2}a_j^3-\tfrac{1}{4}a_j^2-\tfrac{7}{12}a_j+\tfrac{1}{3}+\tfrac{1}{2}a_j^3(a_j+1)\delta_j^2\ln\delta_j] , \quad (33)$$

$$I_j^3=0 , \quad (34)$$

and

$$I_j^4=[\tfrac{1}{2}a_j^2-\tfrac{3}{4}a_j+\tfrac{1}{4}+\tfrac{1}{2}a_j^3\delta_j^2\ln\delta_j] , \quad (35)$$

where the variable δ_j is given by $\delta_j=(M_{\nu(j)}/M_W)^2$ for $j=1,2,3$, and a_j is defined as $a_j=1/(1-\delta_j)$. The sum $I_{\mu e}$ is given by

$$I_{\mu e}=\sum_{j=1}^{3} U_{D_{ej}}U^{\dagger}_{D_{j\mu}}\Lambda_j^2 \times[-\tfrac{3}{2}a_j^3+\tfrac{15}{4}a_j^2-\tfrac{11}{4}a_j+\tfrac{1}{2}-\tfrac{3}{2}a_j^4\delta_j^3\ln\delta_j] . \quad (36)$$

This can be approximated for the two cases where the neutrino masses are all either much less than or much greater than the mass of the W. Thus,

$$\begin{aligned} I_{\mu e} &\simeq \sum_{j=1}^{3} U_{D_{ej}}U^{\dagger}_{D_{j\mu}}\Lambda_j^2\tfrac{1}{4}\delta_j, \quad \text{if all } M_j<M_W , \\ &\simeq \sum_{j=1}^{3} U_{D_{ej}}U^{\dagger}_{D_{j\mu}}\Lambda_j^2\tfrac{1}{2}, \quad \text{if all } M_j>M_W . \end{aligned} \quad (37)$$

Averaging over the initial spins and summing over the final spins and momenta leads to the decay rate

$$\Gamma_{\mu\rightarrow e\gamma}=\frac{\alpha G_F^2 m_{\mu}^5}{128\pi^4}|I_{\mu e}|^2 , \quad (38)$$

where α is the fine structure constant. This can be compared to the decay rate $\Gamma_{\mu\rightarrow e\nu\bar{\nu}}=G_F^2m_{\mu}^5/192\pi^3$ to get the ratio which can then be compared to experiment to get an upper bound on $I_{\mu e}$:

$$\frac{\Gamma(\mu\to e\gamma)}{\Gamma(\mu\to e\nu\bar{\nu})}=\frac{3\alpha}{2\pi}|I_{\mu e}|^2<5\times10^{-11}$$
$$\Rightarrow|I_{\mu e}|<1.2\times10^{-4}$$
$$\Rightarrow\sum_{j=1}^{3}U_{D_{ej}}U^{\dagger}_{D_{j\mu}}\frac{M_{D_j}^2}{M_j^2}<2.4\times10^{-4},\quad\text{if all } M_j>M_W\ . \tag{39}$$

B. $\mu\to ee^+e^-$

This process can occur via extensions of the diagrams in $\mu\to e\gamma$ where the γ is virtual and splits into an electron positron pair; it can take place via a virtual intermediate Z [see Fig. 5(a)] or by box diagrams [see Fig. 5(b)]. It is discussed in Refs. [31,33].

1. Contribution from an intermediate Z

The calculation for the μ-Z-e vertex has effectively been done elsewhere in the context of quark flavor-changing processes. The presentation given here will essentially be that given in Ref. [34]. Figure 5(c) shows the 11 diagrams involved. The calculations are done in the approximation that all the external momenta and masses are zero. Diagrams (1) and (2) show the contribution from the self-energy term for the $\mu-e$ vertex, which arises from loop graphs involving a W or a charged Higgs boson. This contribution is completely canceled (in the approximation that all the external momenta and masses are zero) by the counterterms represented in diagrams (3) and (4). Using dimensional regularization the gauge-invariant counterterm responsible for the cancellation is of the form $\bar{L}_1 i\not{D}L_2$, where L_1 is the left-handed SU(2) doublet containing the electron, L_2 the doublet containing the μ, and D is the gauge-invariant derivative. As well as canceling off the self-energy terms, the counterterm also includes a divergent contribution to the μ-Z-e vertex represented in diagram (5). This divergence is rendered finite when added to the only other divergence, which comes from diagram (11). Diagrams (7), (8), and (9) are completely finite, and diagrams (6) and (8) are finite when summed over all intermediate neutrinos.

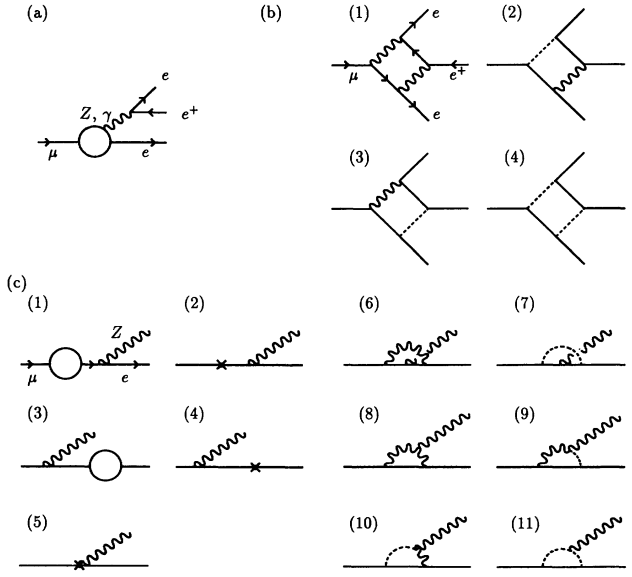

FIG. 5. Feynman diagrams for the flavor changing process $\mu\to ee^+e^-$, Sec. V B. (a) Exchange of a virtual photon or Z. (b) Box diagrams. (c) Diagrams for the μ-Z-e vertex. The circles represent self-energy contributions, the crosses counterterms.

Since three of the intermediate neutrinos are massless, we can define for each of the diagrams i [$i=(5)$–(11)] and each of the intermediate massive neutrinos j ($j=1$–3) a term I_j^i which corresponds to the contribution from the massive neutrino ν_j minus the contribution from a massless neutrino, the total contribution to the μ-Z-e vertex being given by

$$-i\frac{e^3P^-\gamma^\mu}{128\pi^2\sin^3\theta_W\cos\theta_W}\sum_{j=1}^{3}\sum_{i=5}^{11}U_{D_{ej}}U^{\dagger}_{D_{j\mu}}\Lambda_j^2I_j^i\ . \tag{40}$$

Using the same definitions for a_j and δ_j as for the $\mu\to e\gamma$ calculation the I_j^i are calculated to be

$$I_j^5=\delta_j[2(a_j+a_j^2\delta_j\ln\delta_j)+f_5](1-2\sin^2\theta_W)\ , \tag{41}$$
$$I_j^6=\delta_j[-2(a_j+a_j^2\delta_j\ln\delta_j)+4a_j\ln\delta_j]\ , \tag{42}$$
$$I_j^7=\delta_j[2(a_j+a_j^2\delta_j\ln\delta_j)-2]\ , \tag{43}$$
$$I_j^8=\delta_j[-12(1-\sin^2\theta_W)(a_j+a_j^2\delta_j\ln\delta_j)]\ , \tag{44}$$
$$I_j^9=\delta_j[-4(a_j+a_j^2\delta_j\ln\delta_j)]\sin^2\theta_W\ , \tag{45}$$
$$I_j^{10}=\delta_j[-4(a_j+a_j^2\delta_j\ln\delta_j)]\sin^2\theta_W\ , \tag{46}$$
$$I_j^{11}=\delta_j[-(a_j+a_j^2\delta_j\ln\delta_j)+f_{11}](1-2\sin^2\theta_W)\ , \tag{47}$$

where the terms f_5 and f_{11} come from the divergent parts of diagrams (5) and (11). Written in a general dimension d, these terms are given by

$$f_5=\delta_j(a_j+a_j^2\delta_j\ln\delta_j)-\frac{2}{(4-d)}-\Gamma'(1)-\ln\left[\frac{4\pi}{M_W^2}\right]-\frac{1}{2}\ , \tag{48}$$

$$f_{11}=(1-\delta_j)(a_j+a_j^2\delta_j\ln\delta_j)+\frac{2}{(4-d)}+\Gamma'(1)+\ln\left[\frac{4\pi}{M_W^2}\right]+\frac{1}{2}\ . \tag{49}$$

Summing up all the contributions I_j^i from diagrams (5)–(11) and defining I_Z to be the total, we have

$$I_Z = \sum_{j=1}^{3} U_{D_{ej}} U^{\dagger}_{D_{j\mu}} \Lambda_j^2 \delta_j [2(2-7\delta_j) a_j^2 \ln\delta_j - 10 a_j - 2] \ . \tag{50}$$

Notice that, for neutrinos much heavier than M_W, I_Z is entirely dominated by the contribution from an intermediate charged Higgs boson in diagram (7) which contributes the final 2 in the square bracket of the formula above.

By attaching an electron positron pair to the end of the Z we obtain the contribution to the $\mu \to e e^+ e^-$ amplitude from an intermediate Z:

$$\mathcal{A}_Z = iK I_Z \bar{u}_{q1} P^- \gamma_\mu u_p \bar{u}_{q2} [2P^-(-1+2\sin^2\theta_W) + P^+ 2\sin^2\theta_W] \gamma^\mu v_{q-3} \ , \tag{51}$$

where the constant K has the value $K = e^4/256\pi^2 \sin^4\theta_W M_W^2$.

2. Contribution from box diagrams

Figure 5(b) shows all the box diagrams involved. For neutrino masses less than M_W the contribution from box diagram (1) dominates the others. This is due to the fact that the other diagrams involve exchange of virtual charged Higgs bosons whose coupling to the electron and μ is suppressed by a factor of the order of the Dirac mass D over M_W. For neutrino masses larger than M_W the box diagrams involving the exchange of intermediate charged Higgs bosons are negligible in comparison to the contribution from an intermediate Z. This is because the box diagrams with a charged Higgs boson contain two massive neutrinos and are thus suppressed by two sets of mixing angles, as opposed to the single set for the μ-Z-e vertex. For the purposes of our calculation it is therefore only necessary to consider the first box diagram: diagram (1).

The amplitude for the box diagram is calculated using the approximation that all external momenta and masses are zero. The amplitude for the process is

$$\mathcal{A}_\Diamond = -iK I_\Diamond \bar{u}_{q1} P^- \gamma_\eta u_p \bar{u}_{q2} 8 P^- \gamma^\eta v_{q3} \ , \tag{52}$$

where K, as before, has the value $K = e^4/256\pi^2 \sin^4\theta_W M_W^2$ and the dimensionless factor $I_\Diamond$ is

$$I_\Diamond = \sum_{j=1}^{3} U_{D_{ej}} U^{\dagger}_{D_{j\mu}} \Lambda_j^2 \delta_j (a_j - 1 + a_j^2 \ln\delta_j) \ , \tag{53}$$

with the variable δ_j given by $\delta_j = (M_j/M_W)^2$ for $j = 1,2,3$, and a_j defined as $a_j = 1/(1-\delta_j)$.

3. Total amplitude and branching ratio

The contribution to the amplitude from the exchange of a virtual photon is much smaller than the contribution from the box diagrams and the exchange of a Z and so is neglected altogether. The total amplitude can then be written as

$$\mathcal{A}_{\rm tot} = 2K \bar{u}_{q1} P^- \gamma_\eta u_p \bar{u}_{q2} (I^- P^- + I^+ P^+) \gamma^\eta v_{q3} \ , \tag{54}$$

where $I^- = (-1+2\sin^2\theta_W) I_Z - 4 I_\Diamond$ and $I^+ = \sin^2\theta_W I_Z$.

As for the previous flavor-changing process, we can make approximations for the case where all the neutrino masses are less than the mass of the W and where they are all much greater than the mass of the W. We obtain

$$\begin{aligned} I_Z &\simeq \sum_{j=1}^{3} U_{D_{ej}} U^{\dagger}_{D_{j\mu}} \Lambda_j^2 4\delta_j (-3+\ln\delta_j), \quad \text{if all } M_i < M_W \\ &\simeq \sum_{j=1}^{3} U_{D_{ej}} U^{\dagger}_{D_{j\mu}} (\Lambda_j^2 - 2\delta_j), \quad \text{if all } M_i > M_W \ , \end{aligned} \tag{55}$$

$$\begin{aligned} I_\Diamond &\simeq \sum_{j=1}^{3} U_{D_{ej}} U^{\dagger}_{D_{j\mu}} \Lambda_j^2 \delta_j, \quad \text{if all } M_i < M_W \\ &\ll I_Z, \quad \text{if all } M_i > M_W \ . \end{aligned} \tag{56}$$

Averaging $|\mathcal{A}_{\rm tot}|^2$ over the initial spin states and summing over the final spins and momenta lead to the decay rate

$$\Gamma_{\mu \to e e^+ e^-} = \frac{G_F^2 m_\mu^5 \alpha^2}{192\pi^3 256\pi^2 \sin^4\theta_W} (|I^-|^2 + |I^+|^2) \ , \tag{57}$$

where α is the fine structure constant. As before this can be compared to the decay rate $\Gamma_{\mu \to e \nu\bar{\nu}} = G_F^2 m_\mu^5/192\pi^3$ to obtain the ratio which can then be compared to experiment to get a bound on the allowed mass ranges:

$$\begin{aligned} \frac{\Gamma(\mu \to e e^+ e^-)}{\Gamma(\mu \to e \nu\bar{\nu})} &= \frac{\alpha^2}{256\pi^2 \sin^4\theta_W} (|I^-|^2 + |I^+|^2) < 10^{-12} \\ &\Rightarrow (|I^-|^2 + |I^+|^2) < 2.4 \times 10^{-6} \\ &\Rightarrow \sum_{j=1}^{3} U_{D_{ej}} U^{\dagger}_{D_{j\mu}} \frac{M_{D_j}^2}{M_W^2} < 1.3 \times 10^{-3}, \quad \text{if all } M_j > M_W \ . \end{aligned} \tag{58}$$

C. μTi$\to e$Ti

Shanker [35] has performed some careful calculations for μe conversion for different nuclei. These calculations involve using an effective Hamiltonian for the μ-electron-q-q vertex where the q's represent either two up quarks or two down quarks. This effective Hamiltonian is obtained from the same set of diagrams as in the previous section except that the outgoing electron-positron pair are replaced by an incoming and outgoing quark in

the titanium nucleus. The calculation for the amplitude from the previous section can be carried over with a few changes to give an effective Hamiltonian for this interaction:

$$H_{\text{eff}}=\frac{G_F}{\sqrt{2}}\bar{e}P^-\gamma^\lambda\mu 2\sum_{i=0,1}(g_V^{(i)}V_\lambda^{(i)}+g_A^{(i)}A_\lambda^{(i)}) , \tag{59}$$

where $V_\lambda^{(0)}=\frac{1}{2}(\bar{u}\gamma_\lambda u+\bar{d}\gamma_\lambda d)$, $V_\lambda^{(1)}=\frac{1}{2}(\bar{u}\gamma_\lambda u+\bar{d}\gamma_\lambda d)$ are the vector quark currents, and $A_\lambda^{(0)}$ and $A_\lambda^{(1)}$ are the corresponding axial vector currents. The $g_V^{(i)}$ and $g_A^{(i)}$ are constants. Only $g_V^{(0)}$ and $g_V^{(1)}$ are needed for the calculation and they are given by

$$g_V^{(0)}=\frac{\alpha}{16\pi\sin^2\theta_W}(-\tfrac{2}{3}\sin^2\theta_W I_Z-4I_\diamond) , \tag{60}$$

$$g_V^{(1)}=\frac{\alpha}{16\pi\sin^2\theta_W}(2-4\sin^2\theta_W)I_Z . \tag{61}$$

Using the calculations of Shanker [35], we can then obtain the ratio between the decay rate for $\mu\text{Ti}\to e\text{Ti}$ to the rate for μ capture by the nucleus which can be compared to experiment to obtain another bound:

$$\frac{\Gamma(\mu\text{Ti}\to e\text{Ti})}{\Gamma(\mu^-\text{Ti capture})}=265.64|g_V^{(0)}-0.028g_V^{(1)}|^2\le 5\times 10^{-12}$$

$$\Rightarrow|\tfrac{2}{3}\sin^2\theta_W I_Z-4I_\diamond|<2.1\times 10^{-4}$$

$$\Rightarrow\sum_{j=1}^{3}U_{D_{ej}}U_{D_{j\mu}}^\dagger\frac{M_{D_j}^2}{M_W^2}<7.1\times 10, \quad \text{if all } M_j>M_W . \tag{62}$$

The diagrams for the two processes $\mu\text{Ti}\to e\text{Ti}$ and μ capture are essentially the same as the diagrams for $\mu\to ee^+e^-$ and $\mu\to e\nu\bar{\nu}$ but the ratio of the decay rates of the first two processes is much greater than for the second two. Thus, although the bounds placed by experiment on $\mu\text{Ti}\to e\text{Ti}$ are not as strong as those for $\mu\to ee^+e^-$, it is the process $\mu\text{Ti}\to e\text{Ti}$ which places the strongest bounds on the allowed masses.

This difference can be explained by coherence effects. The dominant process for $\mu\text{Ti}\to e\text{Ti}$ leaves the Ti nucleus in its ground state [35], which is a coherent process involving summing the amplitude over all the nucleons. μ capture, on the other hand, is an incoherent process involving summing the square of the amplitude over all the protons.

VI. DISCUSSION AND CONCLUSIONS

One of the desired results of this model was that it would provide a scenario in which weak interaction symmetry breaking could give the neutrinos a mass matrix on a scale similar to that of the electron, μ and τ, while still maintaining massless neutrinos. To investigate this all the plots discussed in this section are marked with a dashed line along which the masses M_{D_i} induced by the mass matrix D (from weak interaction symmetry breaking) are the same as the electron, μ, and τ. For all the plots the excluded regions lie to the left of the curves.

The bounds from Secs. III and IV are plotted separately for each of the Λ_i in Figs. 1–3. To satisfy the scenario in which $M_{D_1}=M_e$, $M_{D_2}=M_\mu$, and $M_{D_3}=M_\tau$ we see that the mass of the third neutrino must be greater than M_W, the second must be heavier than 10 GeV, and the first heavier than 2 GeV.

To examine if there are further restrictions from the flavor-changing processes of Sec. V, the Λ_i have to be plotted on the same graph since the factors $I_{\mu e}$ and $J_{\mu e}$ are functions of all three Λ_i. In fact, because of the very small mixing of the third massive neutrino ν_i^H into the electron and μ neutrinos (the mixing matrix U_D is chosen in this analysis to be like the KM matrix), $I_{\mu e}$, I_Z, and $I_\diamond$ are virtually independent of Λ_3.

Figures 6–8 plot out the constraints from the flavor-changing processes for three different scenarios. They all assumed that the masses M_{D_i} generated by the mass matrix D were in the same ratio as the masses of the electron μ and τ: i.e., $M_{D_1}:M_{D_2}:M_3=M_e:M_\mu:M_\tau$. The dotted line, as before, marks out the line along which the masses M_{D_i} are actually the same as the electron, μ, and τ masses. The flavor-changing processes are plotted alongside all the other constraints from Secs. III and IV. It is immediately clear that flavor-changing processes do not rule out any of the line along which $M_{D_1}=M_e$, $M_{D_2}=M_\mu$, and $M_{D_3}=M_\tau$. The bounds from Z decays and, for the lightest neutrino, meson decays are much more important.

A. Three scenarios

In the scenarios that follow four different ratios of the neutrino masses M_i are considered. The bounds given at the end of the discussion of each scenario assume that $M_{D_1}=M_e$, $M_{D_2}=M_\mu$, and $M_3=M_\tau$.

Scenario 1. Figure 6 $M_1=M_2=M_3$. In Fig. 6 are plots of the allowed regions taking into account all the experimental constraints from Secs. III–V. Areas to the left of the curves are ruled out. The plot is of the mass M_2 of the second heavy neutrino against $1/\Lambda$, the ratio between the two mass scales generated by S and D. The most important constraint comes from the limits set by Z decays on the third neutrino. If they are to lie on the dashed line, all three neutrino masses are constrained to be greater than M_W.

Scenario 2. Figure 7 $M_1:M_2:M_3=1:15:60$. Again,

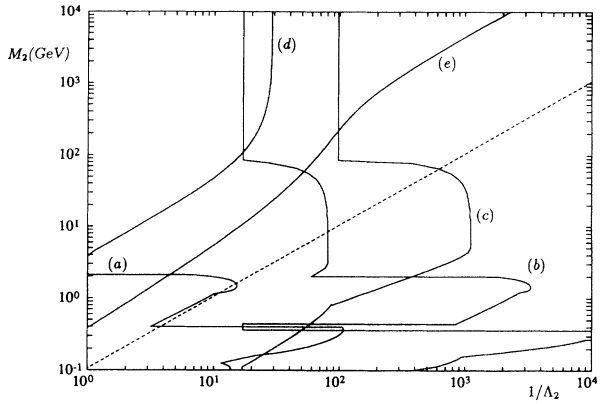

FIG. 6. *Scenario 1.* Regions excluded (to the left of curves) in the M_2, $1/\Lambda_2$ plane from the experimental constraints from Secs. III–V. The ratio between the masses M_{D_1}, M_{D_2}, and M_{D_3} induced by D is $M_{D_1}:M_{D_2}:M_{D_3}=M_e:M_\mu:M_\tau$. The ratio between the masses M_1, M_2, and M_3 is $M_1:M_2:M_3:=1:1:1$. The dashed line corresponds to the line along which $M_{D_1}=M_e$, $M_{D_2}=M_\mu$, and $M_{D_3}=M_\tau$. Regions excluded come from (a) all the restrictions in the $M_1(1/\Lambda_1)$ plane studied in Secs. III and IV; (b) all the restrictions in the $M_2(1/\Lambda_2)$ plane studied in Secs. III and IV; (c) all the restrictions in the $M_3(1/\Lambda_3)$ plane studied in Secs. III and IV; (d) Sec. V A, bounds from $\mu\to e\gamma$; (e) Sec. V C, bounds from $\mu Ti\to eTi$.

areas to the left are ruled out by experiment and the plot is of the mass M_2 of the heaviest neutrino against $1/\Lambda_2$, the ratio between the masses M_2 and M_{D_2}. In this case the most important constraints are those set by D decays on the mass of the first neutrino and those set by Z decays on the mass of the third neutrino. If the masses are

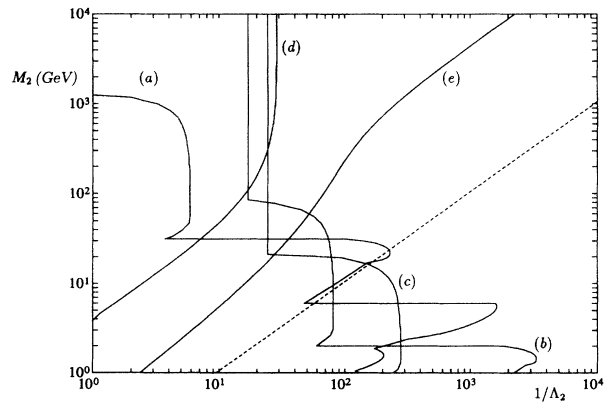

FIG. 7. *Scenario 2.* Regions excluded (to the left of curves) in the $M_2, 1/\Lambda_2$ plane from the experimental constraints from Secs. III–V. The ratio between the masses M_{D_1}, M_{D_2}, and M_{D_3} induced by D is $M_{D_1}:M_{D_2}:M_{D_3}=M_e:M_\mu:M_\tau$. The ratio between the masses M_1, M_2, and M_3 is $M_1:M_2:M_3=1:15:60$. The dashed line corresponds to the line along which $M_{D_1}=M_e$, $M_{D_2}=M_\mu$, and $M_{D_3}=M_\tau$. Regions excluded come from (a) all the restrictions in the $M_1(1/\Lambda_1)$ plane studied in Sec. III and IV; (b) all the restrictions in the $M_2(1/\Lambda_2)$ plane studied in Secs. III and IV; (c) all the restrictions in the $M_3(1/\Lambda_3)$ plane studied in Secs. III and IV; (d) Sec. V A, bounds from $\mu\to e\gamma$; (e) Sec. V C, bounds from $\mu Ti\to eTi$.

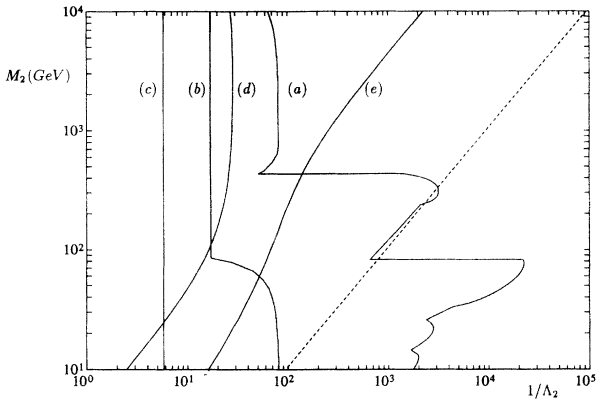

FIG. 8. *Scenario 3.* Regions excluded (to the left of curves) in the M_2, $1/\Lambda_2$ plane from the experimental constraints from Secs. III–V. The ratio between the masses M_{D_1}, M_{D_2}, and M_{D_3} induced by D is $M_{D_1}:M_{D_2}:M_{D_3}=M_e:M_\mu:M_\tau$. The ratio between the masses M_1, M_2, and M_3 is $M_1:M_2:M_3=M_e:M_\mu:M_\tau$. The dashed line corresponds to the line along which $M_{D_1}=M_e$, $M_{D_2}=M_\mu$, and $M_{D_3}=M_\tau$. Regions excluded come from (a) all the restrictions in the $M_1(1/\Lambda_1)$ plane studied in Secs. III and IV; (b) all the restrictions in the $M_2(1/\Lambda_2)$ plane studied in Secs. III and IV; (c) all the restrictons in the $M_3(1/\Lambda_3)$ plane studied in Secs. III and IV; (d) Sec. V A, bounds from $\mu\to e\gamma$; (e) Sec. V C, bounds from $\mu Ti\to eTi$.

to lie on the dashed line, M_2 must be greater than 30 GeV. Dividing this by 15 and multiplying by 4 gives the bounds for the first and third neutrinos, respectively. The bounds for the three neutrinos are thus $M_1>2$ GeV which is equivalent to $M_2>30$ GeV and $M_3>120$ GeV.

Scenario 3. Figure 8 $M_1:M_2:M_3=M_e:M_\mu:M_\tau$. In this scenario it is the constraints set by D decays on the mass of the first neutrino that are most important and the corresponding bounds for the three masses are (for masses lying on the dashed line): $M_1>2$ GeV, $M_2>400$ GeV, and $M_3>3500$ GeV.

B. Conclusions

In this paper we have examined the experimental consequences of a model of massive neutrinos and have excluded a large region of the parameter space. Specifically we have found that, in the scenario where the mass contributions M_{D_i} from weak interaction symmetry breaking are the same as those for the electron, μ, and τ, the neutrino masses are approximately constrained as follows:

$$M_1>2 \text{ GeV}, \quad M_2>10 \text{ GeV}, \quad \text{and } M_3>80 \text{ GeV}. \tag{63}$$

This means that either the Dirac mass connecting standard left-handed neutrinos to right-handed neutrinos has entries less than their charged counterparts, or one would expect reasonably heavy neutrinos. It is clearly nonetheless of interest to improve the bounds. Clearly improved statistics at LEP will give stronger constraints. Furthermore, the bound on M_1 can be improved by looking for heavy neutrinos in B decays.

ACKNOWLEDGMENTS

L.R. thanks CERN and the Rutgers University Physics Department for their hospitality while this work was being completed. This work was supported in part by funds provided by the U.S. Department of Energy (DOE) under Contract No. DE-AC02-76ER03069 and in part by the Texas National Research Laboratory Commission under Grant No. RGFY92C6. L.R. thanks the NSF, the Alfred P. Sloan Foundation and the U.S. DOE for financial support.

[1] C. N. Leung and J. L. Rosner, Phys. Rev. D **28**, 2205 (1983).
[2] D. Wyler and L. Wolfenstein, Nucl. Phys. **B218**, 205 (1983).
[3] L. Randall, Nucl. Phys. **B403**, 122 (1993).
[4] M. Gronau, C. N. Leung, and J. L. Rosner, Phys. Rev. D **29**, 2539 (1984).
[5] D. Britten *et al.*, Phys. Rev. D **46**, 885 (1992).
[6] G. Bernardi *et al.*, Phys. Lett. B **203**, 332 (1988).
[7] G. Bernardi *et al.*, Phys. Lett. **166B**, 479 (1986).
[8] N. De Leener-Rosier *et al.*, Phys. Rev. D **43**, 3611 (1991).
[9] G. Azuelos *et al.*, Phys. Rev. Lett. **56**, 2241 (1986).
[10] D. A. Bryman *et al.*, Phys. Rev. Lett. **50**, 1546 (1983).
[11] T. Yamazaki *et al.*, in *Proceedings of the Eleventh International Conference on Neutrinos and Astrophysics,* Dortmond, West Germany, 1984, edited by K. Klein Knecht and E. A. Paschos (World Scientific, Singapore, 1984), p. 183.
[12] J. Heintz *et al.*, Nucl. Phys. **B149**, 365 (1979).
[13] J. Dorennbosch *et al.*, Phys. Lett. **166B**, 473 (1986).
[14] F. J. Gilman *et al.*, Phys. Rev. D **32**, 324 (1985).
[15] F. Bergsma *et al.*, Phys. Lett. **128B**, 361 (1983).
[16] N. M. Shaw *et al.*, Phys. Rev. Lett. **63**, 1342 (1989).
[17] H.-J. Behrend *et al.*, Z. Phys. C **41**, 7 (1988).
[18] C. Wendt *et al.*, Phys. Rev. Lett. **58**, 1810 (1987).
[19] O. Adriani *et al.*, Phys. Lett. B **295**, 371 (1992).
[20] M. Z. Akrawy *et al.*, Phys. Lett. B **247**, 448 (1990).
[21] Particle Data Group, K. Hikasa *et al.*, Phys. Rev. D **45**, S1 (1992).
[22] M. E. Peskin and T. Takeuchi, Phys. Rev. D **46**, 381 (1992).
[23] G. Czapek *et al.*, Phys. Rev. Lett. **70**, 17 (1993).
[24] T. Goldman and W. Wilson, Phys. Rev. D **15**, 709 (1977).
[25] W. J. Marciano and A. Sirlin, Phys. Rev. Lett. **36**, 1425 (1976).
[26] D. I. Britton *et al.*, Phys. Rev. Lett. **68**, 3000 (1992).
[27] P. Langacker, in *Recent Directions in Particle Theory—From Superstrings and Black Holes to the Standard Model,* Proceedings of the Theoretical Advanced Study Institute in Elementary Particle Physics, Boulder, Colorado, 1992, edited by J. Harvey and J. Polchinski (World Scientific, Singapore, 1993).
[28] R. D. Bolton *et al.*, Phys. Rev. D **38**, 2077 (1988).
[29] U. Bellgardt *et al.*, Nucl. Phys. **B299**, 1 (1988).
[30] S. Ahmad *et al.*, Phys. Rev. D **38**, 2102 (1988).
[31] T. Cheng and L. Li, Phys. Rev. D **44**, 1502 (1991).
[32] G. Altarelli *et al.*, Nucl. Phys. **B125**, 285 (1977).
[33] S. B. Treiman, F. Wilczek, and A. Zee, Phys. Rev. D **16**, 152 (1977).
[34] T. Inami and C. S. Lim, Prog. Theor. Phys. **65**, 297 (1981).
[35] O. Shanker, Phys. Rev. D **20**, 1608 (1979).